Paired Parton Trial States for the Superfluid-Fractional Chern Insulator Transition

Tevž Lotrič and Steven H. Simon
Rudolf Peierls Centre for Theoretical Physics, Parks Road, Oxford, OX1 3PU, United Kingdom

(Received 9 May 2025; revised 17 August 2025; accepted 12 February 2026; published 3 March 2026)

We consider a model of hard-core bosons on a lattice half-filling a Chern band such that the system has a continuous transition between a fractional Chern insulator (FCI) and a superfluid state (SF) depending on the bandwidth to bandspacing ratio. We construct a parton-inspired trial wave function *Ansatz* for the ground states that has remarkably high overlap with exact diagonalization in both phases and throughout the phase transition. Our *Ansatz* is stable to adding some bosonic interactions beyond the on-site hard-core constraint. We confirm that the transition is well described by a projective translation symmetry-protected multiple parton bandgap closure, as has been previously predicted. However, unlike prior work, we find that our wave functions require anomalous (BCS-like) parton correlations to describe the phase transition and SF phase accurately.

DOI: 10.1103/l9rp-y68y

Much of our understanding of fractional quantum Hall (FQH) physics comes from wave functions that have very high overlap with exact diagonalization results. For fractional Chern insulators (FCIs) [1–6], the lattice analog of FQH states, similarly good trial wave functions are known to exist in only a few special cases that can be mapped to a FQH problem—in particular, for so-called ideal [7], or vortexable [8,9], bands with zero bandwidth [10]. In this Letter, we investigate trial wave functions for FCIs suggested by the parton construction for the bosonic $\nu = \frac{1}{2}$ state, demonstrating that they can have very large overlap with the exact ground state, even when the underlying band has significant bandwidth. We show the value of these wave functions by using them to examine a particular phase transition in detail.

The possibility of a continuous transition between a topologically ordered phase and more conventional phases is an interesting aspect of FCI physics that is largely absent for FQH. Understanding conditions under which such transitions can occur could enable easier preparation of many-particle cold-atom FCI states [11–16]. Furthermore, there is fundamental interest in these transitions, as they are examples of transitions beyond the Landau-Ginzburg paradigm. Certain transitions out of topological phases are also predicted to show emergent symmetries absent at the microscopic level [17–19]. Perhaps the clearest example of such a transition is that between the $\nu = \frac{1}{2}$ bosonic FCI and a conventional superfluid (SF), which we study here. After an initial proposal of how a continuous FCI-SF transition may be described within the parton picture [14], there has been some recent work refining the theory [17] and also a recent numerical paper providing evidence for a continuous transition using Density matrix renormalization group (DMRG) techniques [13]. Despite this, it is not clear whether the transition mechanism of Refs. [14,17] is realized in the numerics. Furthermore, the parton picture of this transition relies on a sequence of nontrivial assumptions about the nature of the parton mean-field *Ansatz*, some of which we point out later. It is not immediately obvious if the parton picture leads to a good description of either phase, much less the transition itself. Inspired by the parton picture, we construct a variational wave function *Ansatz,* which we demonstrate to have an excellent overlap with the exact ground state over the entire transition. This answers all of the above concerns: the high overlap gives a solid footing to the parton-based approach, while the parton interpretation of our wave function largely confirms that the transition is of the type discussed by Refs. [14,17]. However, in contrast to previous work on partons, we find that we need to introduce anomalous parton correlators (analogous to BCS theory) to describe the phase transition and SF phase accurately.

Model—A simple system that can display this transition is a lattice of hard-core but otherwise noninteracting bosons half-filling a band with Chern number $\mathcal{C} = 1$. For special lattice models with a nearly flat Chern-band limit, we expect to see a FCI phase, while in a dispersive Chern band, we generically expect a superfluid phase. The presence of the FCI phase is well established, for example, for the *checkerboard* and the *honeycomb* lattice models [13,20–22]. We begin by focusing on these models, so Hamiltonians

of the form

$$H^{\mathrm{B}} = \sum_{\mathbf{x},\mathbf{y}} t(\mathbf{x},\mathbf{y}) b^\dagger(\mathbf{x}) b(\mathbf{y}), \tag{1}$$

together with the hard-core constraint $b(\mathbf{x})^2 = 0$. Here, $\mathbf{x}$ labels lattice sites, and in what follows, the hoppings $t(\mathbf{x},\mathbf{y}) = t^*(\mathbf{y},\mathbf{x})$ are assumed to have lattice translation symmetry, with details for the two models discussed in Sec. I of the Supplemental Material [23].

The parton construction—The FCI state may be described using the parton construction [14,32,33], where we write the bosonic operator as

$$b(\mathbf{r}) = f_1(\mathbf{r}) f_2(\mathbf{r}) \tag{2}$$

with $f_{1,2}$ fermionic operators. This naturally enforces the hard-core constraint $b^2(\mathbf{r}) = 0$, but it doubles the Hilbert space dimension per site. We should concern ourselves only with the physical subspace, where $\hat{n}_1(\mathbf{r}) = \hat{n}_2(\mathbf{r}) = \hat{n}_{\mathrm{B}}(\mathbf{r})$, with $\hat{n}_{1,2}(\mathbf{r}) = f^\dagger_{1,2}(\mathbf{r}) f_{1,2}(\mathbf{r})$ and $\hat{n}_{\mathrm{B}}(\mathbf{r}) = b^\dagger(\mathbf{r}) b(\mathbf{r})$. In a field-theoretical description, this constraint is enforced by coupling the partons to an SU(2) gauge field. The advantage of partonizing is that the parton mean field turns out to describe certain phases, including the FCI, well as it allows us to expand around a nontrivial mean-field point even when $\langle b \rangle = 0$ [32]. In particular, using the parton decomposition Eq. (2) in Eq. (1) and applying the mean-field (MF) approximation, we find up to a constant

$$H^{\mathrm{MF}} = \sum_{\mathbf{x},\mathbf{y}} t(\mathbf{x},\mathbf{y}) \Big[\Big\langle f_1^\dagger(\mathbf{x}) f_1(\mathbf{y}) \Big\rangle_{\mathrm{MF}} f_2^\dagger(\mathbf{x}) f_2(\mathbf{y}) + \Big\langle f_2^\dagger(\mathbf{x}) f_2(\mathbf{y}) \Big\rangle_{\mathrm{MF}} f_1^\dagger(\mathbf{x}) f_1(\mathbf{y}) \Big], \tag{3}$$

where we assumed, for simplicity, that the two partons are independent at the MF level. This assumption is relaxed in Eq. (5). To understand Eq. (3), which is a free Hamiltonian, we need to address a subtlety relating to translational symmetry. We impose that H^{B} is invariant under two bosonic translation operators, $T^{\mathrm{B}}_{1,2}$, which correspond to translations by the primitive lattice vectors and obey $T^{\mathrm{B}}_1 T^{\mathrm{B}}_2 = T^{\mathrm{B}}_2 T^{\mathrm{B}}_1$. We may similarly define translational operators in the parton language $T^{\mathrm{P}}_{1,2}$, but the partons only need to fall into a *projective* representation of this symmetry; in particular, we may have an *Ansatz* where $T^{\mathrm{P}}_1 T^{\mathrm{P}}_2 = -T^{\mathrm{P}}_2 T^{\mathrm{P}}_1$ [32,34]. A physical intuition for this comes from Ref. [14], where a Landau level is considered instead of a lattice $\mathcal{C} = 1$ band. In that case, the unit-charge boson sees 2π flux per plaquette, but Eq. (2) dictates that the two partons share the boson's charge. Assuming they each have half-unit charge, they each see π flux, leading to the above magnetic translation relations for $T^{\mathrm{P}}_{1,2}$, effectively doubling the unit cell. The fact that both partons see equal charge is a nontrivial assumption about the nature of the parton MF state. The success of our approach (below) confirms such an assumption is sensible, but we should note that it is far from guaranteed—for example, for the same Hamiltonian but for filling $\nu = \frac{2}{3}$, the two partons would see *different* charges, and we would get a tripling of the unit cell instead. For $\nu = \frac{1}{2}$, we checked that other extensions of the unit cell do not lead to an improvement in the variational wave function. The magnetic translation relations for $T^{\mathrm{P}}_{1,2}$ mean that the partons see a doubled unit cell, which we take to be generated by the commuting $(T^{\mathrm{P}}_1)^2$ and T^{P}_2 [14,34]. Since the initial problem was at half filling, each flavor of partons fills a band at the MF level. The Chern numbers of these bands determine the phase of the bosonic system. If $t(\mathbf{x},\mathbf{y})$ and the expectation value in Eq. (3) are such that the partons have Chern numbers $\mathcal{C}^{\mathrm{P}}_1 = \mathcal{C}^{\mathrm{P}}_2 = 1$, it can be shown that the system is in a FCI phase. The phase $\mathcal{C}^{\mathrm{P}}_1 = 1, \mathcal{C}^{\mathrm{P}}_2 = 0$ is a Mott insulator, and $\mathcal{C}^{\mathrm{P}}_1 = 1$, $\mathcal{C}^{\mathrm{P}}_2 = -1$ is a superfluid [14]. While the argument in Ref. [14] is field theoretical, much of this may be understood in terms of wave functions.

Let $|\Omega_N\rangle$ be the ground state of Eq. (3) with N partons of each flavor. Given the noninteracting Hamiltonian, $|\Omega_N\rangle$ is a Slater determinant for each parton. Together with Eq. (2), it suggests a bosonic wave function,

$$\phi(\mathbf{r}_1, \ldots, \mathbf{r}_N) = \langle \varnothing | b(\mathbf{r}_1) \ldots b(\mathbf{r}_N) | \Omega_N \rangle. \tag{4}$$

If the parton flavors in $|\Omega_N\rangle$ are independent, this implies that Eq. (4) is the product of two Slater determinants, $\phi(\{\mathbf{r}_j\}) = \det\left[\varphi^{(1)}_k(\mathbf{r}_j)\right] \det\left[\varphi^{(2)}_l(\mathbf{r}_j)\right]$. This is not trivial, however, since both determinants have the same positions as arguments. In the simple case of each parton filling the LLL, each determinant may be written (neglecting Gaussian factors) as $\prod_{i<j}(z_i - z_j)$, and so, Eq. (4) gives $\phi = \prod_{i<j}(z_i - z_j)^2$, the bosonic $\nu = \frac{1}{2}$ Laughlin wave function. Analogously, both partons filling $\mathcal{C}^{\mathrm{P}} = 1$ bands implies a $\nu = \frac{1}{2}$ FCI. The case $\mathcal{C}^{\mathrm{P}}_1 = -\mathcal{C}^{\mathrm{P}}_2$ can be understood by looking at the limit $\varphi^{(2)}_l(\mathbf{r}) = \left(\varphi^{(1)}_l(\mathbf{r})\right)^*$, where it is easy to show that the resulting ϕ has off-diagonal long-range order and represents a superfluid.

Armed with an understanding of the parton description of both phases, Ref. [14] argued that if the effective Hamiltonian, Eq. (3), is varied so that parton 1 remains gapped, while parton 2 undergoes a double Dirac-cone gap closure sending $\mathcal{C}^{\mathrm{P}}_2 = 1 \to -1$, we would have a continuous transition between the FCI $\mathcal{C}^{\mathrm{P}}_2 = 1$ and the SF $\mathcal{C}^{\mathrm{P}}_2 = -1$ states. It was later pointed out that this unusual double gap closure is protected by the projective action of the translation operators on the partons [17–19]. The projective translations guarantee a doubling in the spectrum, as all representations of $T^{\mathrm{P}}_1 T^{\mathrm{P}}_2 = -T^{\mathrm{P}}_2 T^{\mathrm{P}}_1$ are at least two-dimensional. Denoting by $|\psi_{\mathbf{k}}\rangle$ with $\mathbf{k} = (k_x, k_y)$ a one-particle state with eigenvalues e^{ik_x} and e^{ik_y} under $(T^{\mathrm{P}}_1)^2$ and T^{P}_2, we

find that $T_1^{\mathrm{P}}|\psi_{\mathbf{k}}\rangle = |\psi_{\tilde{\mathbf{k}}}\rangle$ with $\tilde{\mathbf{k}} = (k_x, k_y + \pi)$ is degenerate to $|\psi_{\mathbf{k}}\rangle$. So if a gap closure occurs at (q_x, q_y), it must also occur at $(q_x, q_y + \pi)$, implying that the parton Chern numbers jump by two along transitions unless translational symmetry is broken (which is the case when transitioning into the Mott phase). The critical theory of the transition is, then, two gapless Dirac fermions, coupled to an emergent Chern-Simons U(1) gauge field [the initial SU(2) introduced by the partons is assumed to be Higgsed to U(1)] [14].

We again point out that it is far from obvious that this is a physically reasonable scenario. While cylinder DMRG has indeed shown evidence for a continuous transition [13], and it may also be used to probe the predicted SO(3) CDW fluctuation symmetry at the transition [17,18,35], we believe a more direct evaluation of the validity of the parton picture of this transition is necessary. We address these concerns by developing a variational wave function *Ansatz* based on the parton picture and demonstrating superb agreement with other numerical methods. We provide evidence that the transition may indeed be understood as a jump in the parton Chern numbers $\mathcal{C}^{\mathrm{P}}$ in a situation where a double gap closure is protected by the projective action of translations.

We might first try to optimize over all possible *Ansätze* of the determinant-product form described below Eq. (4), as this general form can capture both sides of the transition. While such a procedure sees a transition, we find it to be a relatively poor description of the superfluid phase when comparing to exact diagonalization, as we show in Fig. 1. The reason for this may be traced back to the fact that the partons are assumed independent in the MF state, so $\langle b\rangle_{\mathrm{MF}} = \langle f_1 f_2\rangle_{\mathrm{MF}} = 0$ in that state. Such MF-independent partons can display a superfluid phase [14], but the resulting SF wave function is not accurate. In Sec. III of [23], we develop a field-theoretical picture showing that parton states with a nonzero $\langle f_1 f_2\rangle_{\mathrm{MF}}$ describe the same SF phase and that the MF saddle point generally has a nonzero $\langle f_1 f_2\rangle_{\mathrm{MF}}$. This motivates considering paired parton trial states.

We note here the distinction between the MF and true expectation values—for an operator $\mathcal{O}$ and a MF state $|\Omega\rangle$, we have $\langle\mathcal{O}\rangle_{\mathrm{MF}} = \langle\Omega|\mathcal{O}|\Omega\rangle$, while the true expectation value in the state $|\phi\rangle \propto P|\Omega\rangle$ projected onto the physical subspace [e.g., Eq. (4)], is different. In operator language, $P = \prod_{\mathbf{r}}\{\hat{n}_1(\mathbf{r})\hat{n}_2(\mathbf{r}) + [1-\hat{n}_1(\mathbf{r})][1-\hat{n}_2(\mathbf{r})]\}$. Any valid bosonic operator (including H^{B}) must commute with the projector P [36]. This, together with $P^2 = P$, implies for the projected expectations $\langle\phi|\mathcal{O}|\phi\rangle = \langle\mathcal{O}\rangle = \langle\Omega|\mathcal{O}P|\Omega\rangle/\langle\Omega|P|\Omega\rangle = (\langle\mathcal{O}P\rangle_{\mathrm{MF}}/\langle P\rangle_{\mathrm{MF}})$. The MF expectations evaluate operators on both the physical and unphysical subspaces—still, MF quantities such as Chern numbers are useful to interpret the projected state.

Paired parton states—We choose to work with the most general mean-field *Ansatz*. For K flavors of partons

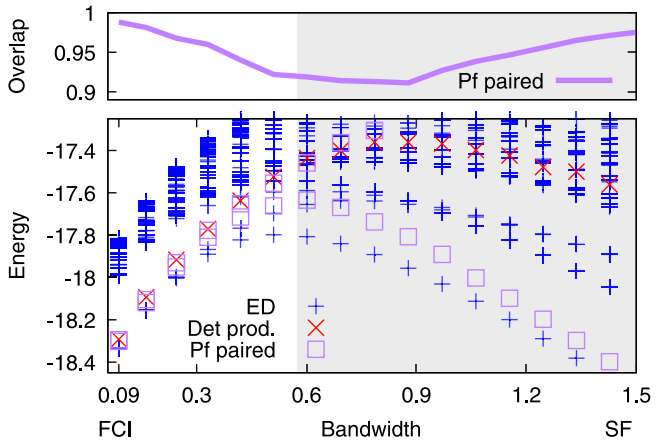

FIG. 1. Comparison of both paired (Pf) and uncorrelated (Det prod.) parton wave function *Ansatz* from VMC against exact diagonalization (ED) in a 9-boson system (total Hilbert space dimension 10^8) as we move from a FCI phase to SF (shaded) by increasing bandwidth. (Top) Overlap of exact ground states with our paired *Ansatz* for the $\mathbf{Q} = (0, 0)$ state, which is the lowest energy branch. (Bottom) Energies of trial states versus ED. Both trial ground states are shown. Deep into the FCI phase, these two are near degenerate, and the Det prod. wave function is also accurate. However, going into the SF phase, the two paired wave functions split, with the $\mathbf{Q} = (\pi, 0)$ and the Det prod. wave functions going up in energy. Note that the gap seen on the SF side is a finite-size effect, while the FCI gap remains finite for large systems. The horizontal axis does not extend down to zero bandwidth, as we would need longer ranged hopping to achieve this.

($K = 2$ in our case), we can write the most general MF Hamiltonian as

$$H^{\mathrm{MF}} = \sum_{\mathbf{x},\mathbf{y}}\sum_{\alpha,\beta=1}^{K} t^{\mathrm{MF}}_{\alpha\beta}(\mathbf{x},\mathbf{y}) f^{\dagger}_{\alpha}(\mathbf{x}) f_{\beta}(\mathbf{y}) + \Delta^{\mathrm{MF}}_{\alpha\beta}(\mathbf{x},\mathbf{y}) f_{\alpha}(\mathbf{x}) f_{\beta}(\mathbf{y}) + \mathrm{H.c.} \tag{5}$$

for some t^{MF}, Δ^{MF}. Considering possible parton contractions in Eq. (1), it may seem that many of the terms in Eq. (5) must be zero. But the operator we should really consider is not H^{B}, but $H^{\mathrm{B}}P$. This will lead to more contractions, possibly over larger distances. While this *allows* for any fermionic bilinear to have a nonzero MF expectation, depending on H^{B}, the best variational wave functions may occur when some bilinears have $\langle\cdot\rangle_{\mathrm{MF}} = 0$. Instead of explicitly evaluating the coefficients in Eq. (5), we note that the ground state, projected to a fixed number of bosons, will always be a Pfaffian. Say we have M partons ($M = 2N$ for N bosons) at positions $\mathbf{r}_j$ and of flavors α_j for $j = 1\ldots M$. Then, the ground state is given by the Pfaffian form [37]

$$\Omega^{\mathrm{MF}}(\{(\mathbf{r}_j, \alpha_j)\}_{j=1\ldots M}) = \mathrm{Pf}[g_{\alpha_j\alpha_k}(\mathbf{r}_j, \mathbf{r}_k)]_{j,k=1\ldots M} \tag{6}$$

for some function $g_{\alpha\beta}(\mathbf{x},\mathbf{y}) = -g_{\beta\alpha}(\mathbf{y},\mathbf{x})$. Due to the possible presence of terms such as $f_1^\dagger f_2$ in Eq. (5), the partons may change flavor. We can think of flavor as an additional site index—each *physical* site $\mathbf{r}$ splits into K subsites indexed by $(\mathbf{r},\alpha)$ for $\alpha = 1\ldots K$. The parton "flavor" then simply specifies at which of these subsites the parton resides. In this language, the physical subspace corresponds to states where each physical site has either all K of its subsites occupied or all of them empty. In our $K = 2$ case, a state with N bosons at positions $\mathbf{r}_1, \ldots, \mathbf{r}_N$ is described by filling both subsites at each of those sites in Eq. (6), giving the bosonic wave function

$$\phi(\{\mathbf{r}_j\}_{j=1\ldots N}) = \Omega^{\mathrm{MF}}(\{(\mathbf{r}_j,1),(\mathbf{r}_j,2)\}_{j=1\ldots N}). \quad (7)$$

This obeys both bosonic statistics and the hard-core constraint. It is equivalent to using a paired MF state $|\tilde{\Omega}\rangle$ in Eq. (4). Our method in what follows is to take the form of Eq. (7) as our wave function *Ansatz*, using the values of the pairing function $g_{\alpha\beta}(\mathbf{x},\mathbf{y})$ as our variational parameters. As ϕ is an *Ansatz* for the full bosonic wave function, the optimization scheme will be to directly minimize $E[\phi] = (\langle\phi|H^{\mathrm{B}}|\phi\rangle/\langle\phi|\phi\rangle)$, bypassing the need to evaluate H^{MF} in Eq. (5). The evaluation of $E[\phi]$ is, however, not analytically tractable, forcing us into variational Monte Carlo (VMC) sampling. Details of the sampling and optimization are shown in the Supplemental Material [23], Sec. IV, and the code is available online [38]. Our VMC procedure is different from any mean-field scheme [e.g., solving Eq. (3) self-consistently], as it optimizes $\langle H^{\mathrm{B}}\rangle = \langle H^{\mathrm{B}}P\rangle_{\mathrm{MF}}/\langle P\rangle_{\mathrm{MF}}$ and not $\langle H^{\mathrm{B}}\rangle_{\mathrm{MF}}$.

We require that the function $g_{\alpha\beta}(\mathbf{x},\mathbf{y})$ in Eq. (6) obeys the translational symmetry mandated by the larger, partonic unit cell [so $(T_1^{\mathrm{P}})^2$ and T_2^{P}]. We do not enforce any action of T_1^{P} itself on $g_{\alpha\beta}(\mathbf{x},\mathbf{y})$—this allows the total bosonic-unit-cell momentum to be $\mathbf{Q} = (0,0)$ and $\mathbf{Q} = (\pi,0)$. By considering $\phi(\{\mathbf{r}\}) \pm \phi(\{\tilde{\mathbf{r}}\})$, with $\{\tilde{\mathbf{r}}\}$ having all particles translated by T_1^{B} relative to $\{\mathbf{r}\}$, we can construct an *Ansatz* for each of the above $\mathbf{Q}$. For system dimensions where the two topologically degenerate states in the FCI phase occur at different momenta, this will allow us to generate both states.

Results and comparison to exact diagonalization—Similarly to Ref. [13], we start with the FCI in the flatband limit of the checkerboard model and vary the hopping parameters (details in Sec. I of [23]) so that the dispersion develops a finite bandwidth with a minimum at the Γ point, $\mathbf{k} = (0,0)$ in the boson Brillouin zone. The magnitude of hopping parameters is $\sim \max(|t|) = 1$ with the bandgap at the same scale. In Fig. 1, we compare our best VMC result to ED for a system of 9 bosons on a 6×3 torus. In the FCI phase, the two topologically degenerate ground states occur at total momenta $\mathbf{Q} = (0,0)$ and $\mathbf{Q} = (\pi,0)$, while the SF phase has a unique GS at $\mathbf{Q} = (0,0)$. Our VMC procedure can find both of the topologically degenerate states. Computing overlaps, our results are remarkable—in a Hilbert space of dimension 10^8, so $\dim\mathcal{H} \sim 5 \times 10^6$ per momentum, we find a 99% overlap in the flatband limit and an overlap $\gtrsim$91% throughout the entire FCI-SF transition for the $\mathbf{Q} = (0,0)$ VMC *Ansatz*. The function $g_{\alpha\beta}(\mathbf{x},\mathbf{y})$ over which we optimize contains $d = 567$ independent parameters. This gives $(\dim\mathcal{H}/d) \sim 10^4$, and the high overlaps indicate that the WF *Ansatz* form captures the physics well. We show energies for both the best paired VMC state at $\mathbf{Q} = (0,0)$ and at $\mathbf{Q} = (\pi,0)$. While the latter is equally good in the FCI limit, it is high in energy in the SF phase because of its momentum. We also show the energies of the determinant-product state, that is, assuming independent partons but still using the full VMC technology. While the energy is good in the flatband limit, and the wave function has only $d' = 54$ parameters, Fig. 1 shows that this *Ansatz* fails to capture the energetics of the SF state, demonstrating the need for the paired *Ansatz*. In Sec. V of the Supplemental Material [23], we also compare our method to the DMRG results of Ref. [13] on the honeycomb lattice, with similar conclusions. While overlaps are considered to be a gold standard for comparison of wave functions to numerics, finite size effects should be treated very carefully. We have seen no indication of behavioral change at larger system sizes, and in Sec. II of the Supplemental Material [23], we show how similar wave functions can be generated for arbitrary system sizes without indication of any new gap closings.

We find numerically that only terms of the form $\langle f_1^\dagger f_1\rangle_{\mathrm{MF}}$, $\langle f_2^\dagger f_2\rangle_{\mathrm{MF}}$, and $\langle f_1 f_2\rangle_{\mathrm{MF}}$ obtain a significant nonzero expectation value. So, while the *Ansatz* Eq. (5) is able to explore a variety of mean-field states, including ones with the gauge group broken to $\mathbb{Z}_2$, our results suggest that states with a U(1) gauge group are favored in this model. Our FCI state is topologically identical to that of Ref. [14]. As discussed in Sec. III of [23], the nonzero $\langle f_1 f_2\rangle_{\mathrm{MF}}$ keeps us in the same SF phase but improves energetics and allows for a larger SF weight. In fact, in Sec. II of the Supplemental Material [23], we show that most of the results in Fig. 1 can be recovered by an explicitly U(1)-invariant short-range parton MF Hamiltonian analogous to Eq. (5).

With a periodic structure in $g_{\alpha\beta}(\mathbf{x},\mathbf{y})$, we may define a MF BdG parton Chern number $\mathcal{C}^{\mathrm{BdG}}$, as discussed in the Supplemental Material [23], Sec. VI. In the limit of decoupled partons, we have $\mathcal{C}^{\mathrm{BdG}} = 2(\mathcal{C}_1^{\mathrm{P}} + \mathcal{C}_2^{\mathrm{P}})$, suggesting $\mathcal{C}^{\mathrm{BdG}} = 4$ for FCI and $\mathcal{C}^{\mathrm{BdG}} = 0$ for SF. A jump of $\mathcal{C}^{\mathrm{BdG}}$ by four units is natural—by the BdG nature, a gap closure at $\mathbf{k}$ implies one at $-\mathbf{k}$, and the projective translation argument then necessitates $\pm\mathbf{k} + (0,\pi)$, generically giving four closures as in Ref. [16]. We observe such a jump at the transition, directly confirming the theoretical proposal of Refs. [14,17] with the transition described by a multiple parton gap closure. But our numerics show that to

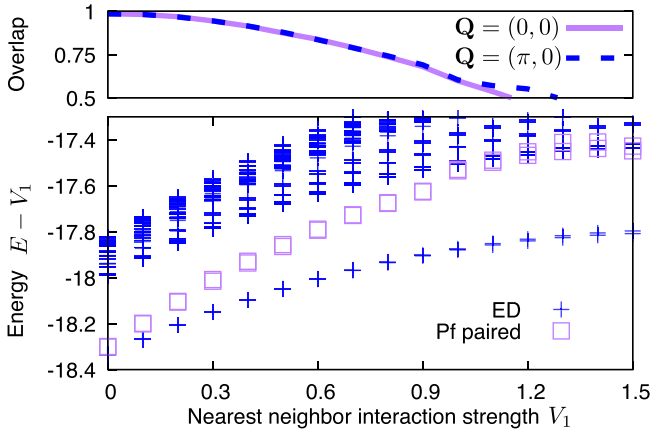

FIG. 2. Energy and overlap comparison of our paired Pf VMC *Ansatz* to exact diagonalization for a finite nearest neighbor repulsion V_1 in the FCI phase at bandwidth 0.09, showing good overlap for both ground states for weak interaction. The overlap becomes worse as V_1 approaches unity, the scale of the hopping parameters and bandgap.

accurately capture the physics, a nonzero anomalous expectation $\Delta = \langle f_1 f_2 \rangle_{\mathrm{MF}}$ must be allowed. While Δ is expected to be zero at the transition in the thermodynamic limit, we argue in Sec. III of [23] that its fluctuations affect details of the transition, including a renormalization of the transition point, which we also observe numerically in an extrapolation to large system sizes.

In Supplemental Material [23], Sec. VII, we present a self-consistent MF method, informed by our above results, which allows us to work with systems large enough to clearly see the quadruple band closure. There are scenarios (explained in detail in Supplemental Material [23], Sec. VI) where $\mathcal{C}^{\mathrm{BdG}}$ can change in steps of 2 *without* breaking translational symmetry, and thus, we can have a phase with $\mathcal{C}^{\mathrm{BdG}} = 2$, which is different from what has been proposed previously, as it can emerge only from a paired-parton *Ansatz*. However, our numerics have not found examples where this is energetically favorable.

We have, so far, considered models with the on-site hard-core constraint being the only interaction. We now add a repulsive density-density interaction $\hat{V} = \frac{1}{2} V_1 \sum_{\langle \mathbf{x},\mathbf{y} \rangle} \hat{n}_{\mathrm{B}}(\mathbf{x}) \hat{n}_{\mathrm{B}}(\mathbf{y})$ between neighboring sites $\langle \mathbf{x}, \mathbf{y} \rangle$. We show the energy and WF overlap agreement with exact results in Fig. 2 as a function of the interaction strength V_1. While the agreement is good for relatively weak $V_1 \lesssim \max(|t|) = 1$, at $V_1 \sim 1$, our trial states have an energy above the gap and a relatively poor ground-state overlap. Throughout the variation, the two topological ground states remain degenerate, and our VMC procedure generates both equally well. Finally, we note that for large V_1, this system approaches a supersolid phase [20,39,40], which may be part of the reason why our *Ansatz* works relatively poorly there.

Conclusions—While it is very satisfying to find that the parton picture, once pairing is allowed, is so successful in describing both the SF and FCI phases as well as the transition between them, it is hard to avoid the question of generalizing this theory to other filling fractions. This could, then, lead to interesting studies of transitions between the $\nu = \frac{1}{3}$ fermionic FCI and various CDW phases [17] or between $\nu = \frac{1}{3}$ FCI and $\nu = \frac{2}{3}$ fermionic FCI, a transition believed to be very similar to the one presented here, but with a tripled parton gap closure and with an emergent SU(3) symmetry [18]. Unfortunately, the overlaps of analogously constructed fermionic FCI wave functions with the exact ground states are not as spectacular. Finding physically motivated generalizations of Eqs. (6) and (7) having better overlap with the ED results would be an interesting future direction.

Note added—Recently, Ref. [35] has appeared online studying the same transition. Our results are consistent where they overlap.

Acknowledgments—We thank the authors of Ref. [13] for sharing some of their DMRG data (replotted in the Supplemental Material [23]). Exact diagonalization computations were performed using the DiagHam library. T. L. acknowledges funding from Leverhulme Trust International Professorship grant (No. LIP-202-014). S. H. S. acknowledges support from EPSRC Grant No. EP/X030881/1.

Data availability—The data that support the findings of this article are openly available [38]; embargo periods may apply.

[1] S. A. Parameswaran, R. Roy, and S. L. Sondhi, Fractional quantum Hall physics in topological flat bands, C.R. Phys. **14**, 816 (2013).

[2] E. J. Bergholtz and Z. Liu, Topological flat band models and fractional Chern insulators, Int. J. Mod. Phys. B **27**, 1330017 (2013).

[3] Z. Liu and E. J. Bergholtz, Recent developments in fractional Chern insulators, in *Encyclopedia of Condensed Matter Physics* (2nd ed.), edited by T. Chakraborty (Academic Press, Oxford, 2024), pp. 515–538.

[4] H. Park, J. Cai, E. Anderson, Y. Zhang, J. Zhu, X. Liu, C. Wang, W. Holtzmann, C. Hu, Z. Liu, T. Taniguchi, K. Watanabe, J.-H. Chu, T. Cao, L. Fu, W. Yao, C.-Z. Chang, D. Cobden, D. Xiao, and X. Xu, Observation of fractionally quantized anomalous Hall effect, Nature (London) **622**, 74 (2023).

[5] F. Xu, Z. Sun, T. Jia, C. Liu, C. Xu, C. Li, Y. Gu, K. Watanabe, T. Taniguchi, B. Tong, J. Jia, Z. Shi, S. Jiang, Y. Zhang, X. Liu, and T. Li, Observation of integer and fractional quantum anomalous Hall effects in twisted bilayer $MoTe_2$, Phys. Rev. X **13**, 031037 (2023).

[6] Z. Lu, T. Han, Y. Yao, A. P. Reddy, J. Yang, J. Seo, K. Watanabe, T. Taniguchi, L. Fu, and L. Ju, Fractional quantum anomalous Hall effect in multilayer graphene, Nature (London) **626**, 759 (2024).
[7] R. Roy, Band geometry of fractional topological insulators, Phys. Rev. B **90**, 165139 (2014).
[8] P. J. Ledwith, A. Vishwanath, and D. E. Parker, Vortexability: A unifying criterion for ideal fractional Chern insulators, Phys. Rev. B **108**, 205144 (2023).
[9] M. Fujimoto, D. E. Parker, J. Dong, E. Khalaf, A. Vishwanath, and P. Ledwith, Higher vortexability: Zero-field realization of higher Landau levels, Phys. Rev. Lett. **134**, 106502 (2025).
[10] E. Kapit and E. Mueller, Exact parent hamiltonian for the quantum Hall states in a lattice, Phys. Rev. Lett. **105**, 215303 (2010).
[11] J. Motruk and F. Pollmann, Phase transitions and adiabatic preparation of a fractional Chern insulator in a boson cold-atom model, Phys. Rev. B **96**, 165107 (2017).
[12] T.-S. Zeng, Phase transitions of bosonic fractional quantum Hall effect in topological flat bands, Phys. Rev. B **103**, 085122 (2021).
[13] H. Lu, H.-Q. Wu, B.-B. Chen, and Z. Y. Meng, Continuous transition between bosonic fractional Chern insulator and superfluid, Phys. Rev. Lett. **134**, 076601 (2025).
[14] M. Barkeshli and J. McGreevy, Continuous transition between fractional quantum Hall and superfluid states, Phys. Rev. B **89**, 235116 (2014).
[15] A. S. Sørensen, E. Demler, and M. D. Lukin, Fractional quantum Hall states of atoms in optical lattices, Phys. Rev. Lett. **94**, 086803 (2005).
[16] M. Barkeshli, N. Y. Yao, and C. R. Laumann, Continuous preparation of a fractional Chern insulator, Phys. Rev. Lett. **115**, 026802 (2015).
[17] X.-Y. Song, Y.-H. Zhang, and T. Senthil, Phase transitions out of quantum Hall states in moiré materials, Phys. Rev. B **109**, 085143 (2024).
[18] J. Y. Lee, C. Wang, M. P. Zaletel, A. Vishwanath, and Y.-C. He, Emergent multi-flavor QED_3 at the plateau transition between fractional Chern insulators: Applications to graphene heterostructures, Phys. Rev. X **8**, 031015 (2018).
[19] X.-Y. Song and Y.-H. Zhang, Deconfined criticalities and dualities between chiral spin liquid, topological superconductor and charge density wave Chern insulator, SciPost Phys. **15**, 215 (2023).
[20] Y.-F. Wang, Z.-C. Gu, C.-D. Gong, and D. N. Sheng, Fractional quantum Hall effect of hard-core bosons in topological flat bands, Phys. Rev. Lett. **107**, 146803 (2011).
[21] T. Neupert, L. Santos, C. Chamon, and C. Mudry, Fractional quantum Hall states at zero magnetic field, Phys. Rev. Lett. **106**, 236804 (2011).
[22] K. Sun, Z. Gu, H. Katsura, and S. Das Sarma, Nearly flatbands with nontrivial topology, Phys. Rev. Lett. **106**, 236803 (2011).
[23] See Supplemental Material at http://link.aps.org/supplemental/10.1103/l9rp-y68y for additional calculation details, which include Refs. [24–31].
[24] M. E. Peskin, Mandelstam-'t Hooft duality in Abelian lattice models, Ann. Phys. (N.Y.) **113**, 122 (1978).
[25] C. Dasgupta and B. I. Halperin, Phase transition in a lattice model of superconductivity, Phys. Rev. Lett. **47**, 1556 (1981).
[26] N. Seiberg, T. Senthil, C. Wang, and E. Witten, A duality web in $2+1$ dimensions and condensed matter physics, Ann. Phys. (Amsterdam) **374**, 395 (2016).
[27] G. J. Henderson, G. Möller, and S. H. Simon, Energy minimization of paired composite fermion wave functions in the spherical geometry, Phys. Rev. B **108**, 245128 (2023).
[28] G. Carleo and M. Troyer, Solving the quantum many-body problem with artificial neural networks, Science **355**, 602 (2017).
[29] D. P. Kingma and J. Ba, Adam: A method for stochastic optimization, arXiv:1412.6980.
[30] R. G. Xu, T. Okubo, S. Todo, and M. Imada, Optimized implementation for calculation and fast-update of Pfaffians installed to the open-source fermionic variational solver mVMC, Comput. Phys. Commun. **277**, 108375 (2022).
[31] T. Fukui, Y. Hatsugai, and H. Suzuki, Chern numbers in discretized brillouin zone: Efficient method of computing (spin) Hall conductances, J. Phys. Soc. Jpn. **74**, 1674 (2005).
[32] X.-G. Wen, *Quantum Field Theory of Many-Body Systems: From the Origin of Sound to an Origin of Light and Electrons* (Oxford University Press, New York, 2007).
[33] X.-G. Wen, Projective construction of non-Abelian quantum Hall liquids, Phys. Rev. B **60**, 8827 (1999).
[34] J. McGreevy, B. Swingle, and K.-A. Tran, Wave functions for fractional Chern insulators, Phys. Rev. B **85**, 125105 (2012).
[35] T. Wang, X.-Y. Song, M. P. Zaletel, and T. Senthil, Emergent QED_3 at the bosonic laughlin state to superfluid transition, arXiv:2507.07611.
[36] This translates to requiring $\mathcal{O}$ to be a singlet with respect to the SU(2) gauge field in the field-theoretical approach.
[37] N. Read and D. Green, Paired states of fermions in two dimensions with breaking of parity and time-reversal symmetries and the fractional quantum Hall effect, Phys. Rev. B **61**, 10267 (2000).
[38] A Julia implementation of the VMC code is publicly available online, https://github.com/tevz-lotric/VMCpartonTrialWF.
[39] W.-W. Luo, A.-L. He, Y. Zhou, Y.-F. Wang, and C.-D. Gong, Quantum phase transitions in a $\nu = \frac{1}{2}$ bosonic fractional Chern insulator, Phys. Rev. B **102**, 155120 (2020).
[40] H. Lu, H.-Q. Wu, B.-B. Chen, and Z. Y. Meng, Vestigial gapless boson density wave emerging between $\nu = 1/2$ fractional Chern insulator and finite-momentum supersolid, Phys. Rev. B **113**, 035141 (2026).